Journal of Green Economy and Low-Carbon Development
https://www.acadlore.com/journals/JGELCD

Improved Ant Colony Optimization for Food Supply Chain Networks: To Achieve the "Dual Carbon" Goals from the Green Perspective

Yuanyuan Zhang*, Xuhan Zhang, Zheyao Li, Nuoning Zheng, Xianglong Li, Zirong Gan, Xiao Li, Yuxin Xue

College of Transportation and Civil Engineering, Fujian Agriculture and Forestry University, 350002 Fuzhou, China

* Correspondence: Yuanyuan Zhang (zhangyy@fafu.edu.cn)

Received: 08-15-2025 **Revised:** 09-17-2025 **Accepted:** 09-23-2025

Citation: Y. Y. Zhang, X. H. Zhang, Z. Y. Li, N. N. Zheng, X. L. Li, Z. R. Gan, X. Li, and Y. X. Xue, "Improved ant colony optimization for food supply chain networks: To achieve the "Dual Carbon" goals from the green perspective," *J. Green Econ. Low-Carbon Dev.*, vol. 4, no. 3, pp. 160–175, 2025. https://doi.org/10.56578/jgelcd040303.

Abstract: Against the backdrop of the "Dual Carbon" goals and the global green transformation of supply chains, the food supply chain characterized by high carbon emissions, significant losses, and stringent time-sensitive requirements imperatively transitions from the traditional "efficiency-first" model to a "dual-driven, efficiency-low carbon" approach. There is a scarcity of existing research to address the limitations encountered in the optimization of single transportation mode and the coordination of multiple constraints. In this light, the current paper focused on the two-stage location-route problem, in order to construct a collaborative optimization model that integrates the location selection of transfer stations with route planning. By dynamically determining the layouts of transfer stations via an enhanced K-means clustering algorithm and introducing capacity constraints and moment of inertia analysis, the accuracy of site selection could be improved. This approach resolved issues of random initialization and load imbalance inherent in traditional clustering. The design of an adaptive ant colony optimization (ACO) algorithm could incorporate heuristic information such as load utilization rate and time window tightness, while optimizing the pheromone update mechanism to balance transportation costs, carbon emissions, and time constraints. The proposed collaborative delivery model effectively integrated the economies of scale from trunk transportation with the flexibility of last-mile delivery, so as to achieve optimization of facility locations and route planning. Experimental validation demonstrated that the improved algorithm significantly outperformed traditional methods in the quality and stability of solutions. It also provided an optimized path for food supply chain networks that balanced economic and environmental benefits. This research offers theoretical support for the transformation of green logistics; it can also be extended to future studies by incorporating real-time data and dynamic scenarios for effective carbon reduction across the entire supply chain.

Keywords: Food supply chain; Two-level location-route problem; K-means algorithm; Ant colony optimization; Constraints

1 Introduction

As the core foundation supporting the efficient operation of the national economy, the logistics industry seamlessly integrates commodity circulation, information transmission, and resource allocation. It tightly connects the production, distribution, exchange, and consumption segments, to establish a multi-dimensional collaborative network spanning regions and industries to safeguard the development of all sectors. In the development of the real economy, the logistics sector not only fulfills the fundamental functions of services such as reducing corporate inventory costs and shortening market response cycles, but also significantly enhances the resilience of industrial and supply chains through innovative models like optimizing multimodal transport systems and deploying smart warehousing networks. Although the logistics industry in China started relatively late, it has entered a new phase of high-quality development driven by both the digital economy and industrial upgrading. Infrastructure networks continue to improve; smart technologies are widely applied, and supply chain service systems are accelerating the construction, thus achieving systematic progress toward standardization, intensification, and greening. In 2024, the total social logistics volume of China reached 360.6 trillion yuan, marking an increase of 8.2 trillion yuan, or 2.3%, compared to 2023. Figure 1 presents the statistics of China's total social logistics volume from 2016 to 2024. The

chart demonstrates steady annual growth in recent years. Although the year-on-year growth rate slowed down in 2020 due to the pandemic, the upward trend remained intact.

The statistics on the total social logistics volume from 2016 to 2024 in China are as follows:

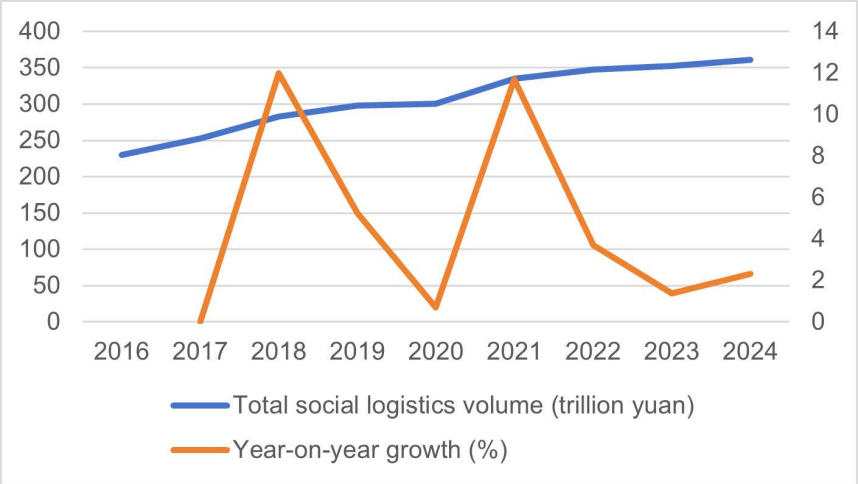

Figure 1. Statistical data of the total social logistics volume in China from 2016 to 2024

In the broader transition of the logistics industry towards greener and smarter operations, the unique characteristics of the food supply chain position it as a critical frontier in the drive towards low carbonization. As a significant component of total social logistics, data from the China Federation of Logistics & Purchasing for 2024 indicated that food distribution accounted for 68% of the total logistics volume for agricultural products. The intensity of cold chain transportation for food was 3 to 5 times of ordinary goods; carbon emissions generated during storage and transportation accounted for approximately 22% of the total emissions across the entire logistics sector. In the sector of fresh agricultural products, annual losses exceeding 200 billion yuan nationwide resulted from cold chain disruptions, equivalent to 12 million tons of additional carbon dioxide emissions. With the introduction of policy documents such as the Green Food Supply Chain Construction Guidelines, the food supply chain is undergoing a shift from the traditional "efficiency-first" approach to a "dual-drive" model, which emphasizes both efficiency and low-carbon practices. This transformation not only responds to the inherent need for quality improvement and efficiency gains amid the sustained growth of total social logistics volume, but also provides a practical pathway for realizing the objectives of the 14th Five-Year Plan for logistics development.

Foreign scholars began researching the optimization of food supply chains relatively early, resulting in well-established theoretical frameworks. Most international researchers nowadays focused on optimizing supply chains from a technical perspective, while actively integrating green concepts and striving to embed sustainable development practices throughout every stage of supply chain management. By integrating the fuzzy best-worst method with the Technique for Order of Preference by Similarity to Ideal Solution (TOPSIS), a scenario-based robust optimization model was proposed to effectively reduce the total supply chain costs while minimizing carbon emissions [1]. A mixed-integer linear programming model was designed for a green and resilient closed-loop supply chain network. A novel four-valued refined multi-objective neutral optimization algorithm was introduced to solve the model, in order to achieve an optimal balance among cost, greenhouse gas emissions, and resilience [2]. Employing a rigorous two-stage stochastic optimization approach, a thorough multi-stage and multi-period green supply chain design model was developed to manage parameter uncertainty and disruptions. The model achieves the minimization of disruption costs and carbon emissions [3]. A multi-stakeholder framework has been developed to identify and evaluate the drivers for the adoption and implementation of carbon regulation policies within manufacturing supply chains, with an aim to enhance ecological sustainability [4]. Seeking insights from manufacturing experts to understand how sustainable integration with lean innovation can support manufacturing supply chains in achieving net-zero emissions and becoming more environmentally friendly. Furthermore, employing a robust two-step approach involving powerful order data envelopment analysis and machine learning-based Bayesian networks ultimately reveals that organizational incentive programs, the availability of expertise, and the accessibility of funding for implementing sustainable practices are critical to organizational transformation and carbon neutrality [5].

The integrated application of drones in parcel delivery represents an innovative logistics solution, wherein trucks serve both as transport vehicles and drone take-off/landing platforms. This research focused on urban truck-drone collaborative delivery, to construct a time-dependent vehicle routing problem with drone (TDVRP-D) mixed-integer programming model, which could minimize transport costs and truck carbon emissions. The proposed meta-

heuristic algorithm based on visual neural networks outperformed existing methods in both the quality of solution and computational efficiency, thus proving particularly suitable for large-scale scenarios [6]. Bicycle-sharing delivery routes undergo adjustments to accommodate demand diversion in high-traffic areas such as transport hubs. This study addressed the challenge of carbon-aware path planning under vehicle load constraints by establishing a model that simultaneously minimizes both carbon emissions and delivery costs. A genetic algorithm (GA) was designed, with analyses conducted on its time complexity and approximation bounds. Empirical testing using data from Yanta District in Xi'an achieved an approximation ratio of 3.52 [7] and thus validated the effectiveness of the algorithm. As a major contributor to energy consumption and carbon emissions, the logistics sector urges for green development. This study identified a low-carbon vehicle routing problem that accounted for high-granularity time-dependent speeds, speed fluctuations, road conditions, and time windows. It employed a Graph Convolutional Network (GCN) model to predict the traffic speeds for precise assessment of carbon emissions, and introduced a hybrid genetic algorithm incorporating adaptive variable neighborhood search. Case studies in Jingzhou validated the effectiveness of this methodology [8].

Research on the design of supply chain optimization by Chinese scholars commenced relatively late, as current studies predominantly focused on optimizing the supply chain network from a green perspective for industrial applications. Given the significant contribution of food supply chains to global greenhouse gas emissions, gaining a thorough understanding of their carbon footprints is of paramount importance. Against the backdrop of low-carbon transition, green supply chains are accelerating their restructuring and evolution. This paper examined the current state, challenges, and opportunities of global green supply chains driven by circular innovation in renewable resources, via adopting the perspective of mineral resource supply. Integrating the context of China's national waste recycling system development, it holds significantly practical relevance and scientific value, thus providing foundational pathways for medium-to-long-term advancement [9]. Under the supply chain spillover effect, digital technological innovations of clients transmit through capital and innovation spillovers to suppliers. Based on the data of Shanghai and Shenzhen A-share from 2008 to 2021, carbon emissions of suppliers were significantly curbed by enhancing profit cash flows, alleviating financing constraints, and promoting green innovation. This effect proved more pronounced under specific corporate characteristics, placing much emphasis on the promotion of corporate digital innovation and the refinement of supply chain coordination mechanisms [10]. Against the backdrop of national green transition, this paper examined how carbon emission trading mechanisms influenced green innovation through bottom-up transmission in supply chains. Findings revealed that when customers were incentivized by such mechanisms, they drove suppliers' green innovation via dual pressure and incentive mechanisms. This propelled suppliers towards substantive innovation and fostered digital technology-enabled innovation, with suppliers in high-carbon industries exhibiting more pronounced responses. This research provided evidence for the "Porter Hypothesis" from the supply chain perspective, in order to offer insights for deepening carbon market development and advancing the green transformation of supply chains [11]. To reduce carbon emissions, a secondary supply chain involving the participation and coordination of the government has been established. Research and analysis have examined the impact of carbon trading prices and government-driven factors on carbon reduction and pricing decisions of the supply chain. Findings indicated that for corporate supply chains, emphasis should be placed on the reduction of low-carbon emissions to enhance corporate motivation to reach such a target [12]. The synergistic dual transformation represents a pivotal measure for achieving carbon peaking and carbon neutrality, advancing openness to the outside world, and fostering ecological development. To investigate their impact on green and low-carbon innovation in export enterprises, this study examined non-financial listed companies on the Shanghai and Shenzhen stock exchanges from 2011 to 2022. Findings indicated that synergistic transformation significantly promoted such innovation as verified, with more pronounced effects observed in specific enterprises. This transformation exerts influence through five dimensions and exhibits varying impacts on supply chains, thereby offering practical insights for relevant implementation [13]. This paper constructed decision models for three scenarios involving green design and green marketing among supply chain members, to analyze the effects of green design costs/demand and green marketing efforts. Findings indicated that increasing these effects tended to enhance green design and marketing efforts, while improving the performance of the supply chain though it does not necessarily reduce the overall environmental impact of products [14]. Under the "Dual-Carbon" goals and heightened environmental awareness, green mergers and acquisitions represent a crucial strategy for high-polluting enterprises to address compliance pressures and enhance the resilience of the supply chain. Empirical analysis of the listed companies in this sector from 2012 to 2023 demonstrated that such initiatives yielded tangible outcomes through mechanisms like green reputation, technological innovation, and green investment. Notably, enterprises exhibiting willingness of high disclosure and government subsidies received under the "Dual-Carbon" framework achieve more pronounced effects, with significant contributions in carbon reduction. This study expanded relevant perspectives and provided empirical support [15].

Research on the optimization design of supply chain network has been increasingly focusing on the critical area of collaborative delivery. Not only does it significantly enhance the operational efficiency of the supply chain,

but also serves as the core driving force propelling supply chain network optimization to new heights. Booming e-commerce and emergency logistics have raised demands for efficient and flexible delivery, which traffic-constrained traditional models struggle to meet. This study developed an integrated multi-truck multi-drone system as a mixed-integer nonlinear program (MINLP) model (linearized to MILP for solvability), featuring bidirectional logistics, multi-mission drones, time windows, payload-dependent energy, and no-fly zone rerouting. Having tested on 16 Seattle/Buffalo datasets, an adaptive large neighborhood search (ALNS) algorithm optimizes large-scale cases and the model cuts costs/time vs. truck-only/non-detour schemes, with sensitivity analyses to confirm its adaptability for urban low-altitude logistics [16]. This study formulated a randomized truck-drone collaborative delivery problem, in order to minimize transport costs by optimizing car park locations, planning of truck routes, and store allocation. Constraints include load capacity limits, restrictions of drone range, time window requirements, and uncertainty in demand/travel times. A two-stage stochastic model (incorporating deterministic reconstruction) and an enhanced scenario decomposition algorithm were proposed. Algorithm performance, value of randomization, and influences of key parameters were validated using two datasets [17]. Against the backdrop of burgeoning e-commerce and underutilized ground relay point (RP) infrastructure, this study proposed the Relay Point-Enhanced Collaborative Truck-Drone Delivery Model (RPECTDDM). By integrating a mixed-integer linear programming (MILP) model with a two-stage adaptive network selection (ALNS) algorithm, it optimized relay point selection, customer allocation, and route planning. During validation in Chengdu, this approach outperformed three benchmark schemes (achieving up to 48.47% cost savings compared to Train Once Deploy Many (TODM)). Sensitivity analysis revealed that costs of relay points and drone endurance capacity critically influenced the effectiveness of the scheme [18]. E-commerce and environmental pressures are driving logistics enterprises to upgrade their delivery systems. The collaborative operation of drones and lorries has overcome the limitations of drone-only models. The current paper analyzed 15 literature reviews and 144 studies on lorry-drone last-mile delivery, in order to categorize challenges and solutions, identify research gaps, and propose future directions to advance this innovative logistics model. Driven by the growth of e-commerce, the logistics industry faces multiple challenges including high costs, extended delivery time, and labor shortages. This study proposed the Truck-Drone Collaborative Delivery Routing Problem (TDCRPTW) multi-objective optimization model, which achieved multi-vehicle-drone collaborative delivery by minimizing costs and maximizing delivery reliability within capacity/time window constraints. Having solved via a two-stage strategy (adaptive K-means+++TCMSA), experiments validated that this model delivered 10% to 50% cost reductions and 15% to 40% of time savings, thus offering significant insights for enhancing the efficiency of e-commerce logistics [19]. Unmanned aerial vehicles (UAVs) demonstrate significant potential in emergency response within regions with inadequate road infrastructure, yet remain constrained by limited battery capacity. While hybrid truck-UAV systems address this limitation, fixed-mount configurations compromise UAV operational flexibility. This study proposed a Dynamic Team-Based Decoupling (DTDC) strategy, which mathematically decomposes the scheduling task into three distinct phases: Demand allocation, truck route planning, and drone dispatch. Empirical results demonstrated that this strategy outperformed existing state-of-the-art solvers and meta-heuristic algorithms [20].

A review of existing literature revealed that scholars both domestically and internationally conducted multifaceted research on optimizing food supply chains, so as to achieve significant outcomes in the areas of environmental sustainability and green development. Nevertheless, current studies remain subject to certain limitations. This design addressed the critical junctures and core challenges concerning carbon emissions within the networks of food supply chain. It aims to implement a coordinated delivery model combining lorries and drones, based on a thorough assessment of the multiple cost factors involved in the supply chain and the scientific selection of the most suitable transport mode.

2 Description of the Problem and Model Assumptions

2.1 Description of the Problem

The Two-Echelon Location-Routing Problem (2E-LRP) studied in this paper can be broadly described as a multi-objective logistics network optimization problem that minimizes total costs by comprehensively considering constraints such as selection of hub locations, two-stage route planning, food spoilage, and carbon emissions.

First, based on the distribution of all customer points within the region, demand scale, and specific requirements for food timeliness, a layout plan for distribution hubs was carefully selected and determined from numerous candidate locations. This plan specified the number, coordinates, and service capacity of the hubs. During this process, customer points were assigned to different hubs in accordance with spatial proximity, demand matching, and food shelf life. Each customer point was strictly served by only one hub, and the total demand handled by each hub did not exceed its capacity limit, thus ensuring orderly delivery operations.

Next, based on the actual customer demand, the required distribution hubs were dynamically activated. Primary transport vehicles departed from the distribution center and carried goods to each hub via trunk routes. This process strictly adhered to weight constraints, while fully considering requirements of food timeliness and planning optimal routes to ensure goods arrived at hubs quickly and safely within their shelf life. Secondary transport vehicles departed

from these hubs after planning for the last-mile delivery routes precisely. They had to satisfy customers' demands for food, while ensuring that the delivery time was aligned with customer time window requirements, and each customer's demand did not exceed the load capacity of the secondary vehicle.

This problem achieved overall optimization through a two-stage approach: Stage One determined hub locations by balancing efficient customer coverage with costs of carbon emissions and impacts of food timeliness. Stage Two coordinated two-tier vehicles to execute the entire "trunk-to-last-mile" operation through integrating carbon emission costs, transportation expenses, and food timeliness requirements as core optimization objectives during route planning. The ultimate goal is to minimize the total costs of the system, including hub construction expenses, two-tier transportation expenses, carbon emission costs, and potential losses from food delays while satisfying all constraints. This approach significantly enhances the overall operational efficiency of the food supply chain network, hence achieving a balanced integration of economic benefits, environmental benefits, and food quality assurance.

2.2 Symbols and Assumptions

The explanation of the symbols and definition of the parameters are as shown in Tables 1 and 2.

Table 1. Descriptions of the symbols

Symbol	Definition
I	Candidate hub set
J	Customer point set
K_1	Primary vehicle set
K_2	Primary vehicle set
T	Time period set during the planning period

Table 2. Definition of parameters

Parameter	Definition
d_{ij}	Distance between candidate transit hub i and customer point j
d_{0j}	Distance between distribution center and candidate transfer hub j
q_j	Customer demand for food items at point j
C_i	Capacity of candidate transit hub i
f_i	Fixed cost for construction and operation of candidate transit hub i
V_{k_1}	Travel speed of level 1 transport vehicle k_1
V_{k_2}	Travel speed of secondary carrier k_2
λ_{k_1}	Carbon emission factor for primary transport mode k_1 (per unit distance)
λ_{k_2}	Carbon emission factor for secondary transport vehicle k_2 (per unit distance)
C_{k_1}	Unit distance transportation cost of primary carrier k_1
C_{k_2}	Unit transportation cost per distance for secondary carrier k_2
a	Food loss rate
h_j	Time window requirements for customer orders at point j (earliest & latest delivery times)
Q_{k_1}	Maximum payload capacity of level 1 transport vehicle k_1
Q_{k_2}	Maximum payload capacity of secondary carrier k_2

2.2.1 Basic assumptions of the model

(1) Assume the geographical locations of distribution centers, transfer hubs, and customer points are known and fixed;

(2) Delivery vehicles maintain constant speeds, disregarding traffic congestion, weather, and other factors affecting the time for travel;

(3) Food spoilage during transportation and storage depends solely on time, with a known constant spoilage rate;

(4) Primary and secondary transport vehicles are fixed types with known parameters, such as load capacity and factors of carbon emissions;

(5) Fixed costs (e.g., construction and operational expenses) for candidate transfer hubs are known, and their capacity remains constant throughout the planning period once selected for construction;

(6) A single secondary delivery vehicle can carry multiple parcels per trip;

(7) The cargo demand at a distribution transfer station equals the total demand from customers within its cluster;

(8) Secondary logistics network delivery services can only commence after primary delivery vehicles have completed their service to all distribution hubs within that network; and

(9) Each secondary delivery vehicle departing from a distribution hub must return to the same distribution hub.

2.2.2 Specifications of the constraints

(1) Customer Demand Fulfillment Constraint: Ensure that every customer's food order is fulfilled, namely:

$$\sum_{i \in I} y_{ij} = 1, \quad \forall \mathrm{j} \in J \tag{1}$$

(2) Capacity Constraints of Transfer Hubs: The total service demand at a transfer hub must not exceed its capacity limit and is expressed as:

$$\sum_{j \in J} q_j y_{ij} \leq C_i x_i, \quad \forall i \in I \tag{2}$$

(3) Payload Constraints of Transport Vehicles: Ensure that the total cargo transported by each primary transport vehicle does not exceed its payload limit and can be expressed as:

$$\sum_{i \in I} q_j y_{ij} z_{ikl} \leq Q_{kl}, \quad \forall k_l \in K_l \tag{3}$$

Ensure that the cargo volume delivered by each secondary transport vehicle does not exceed its rated load capacity and can be expressed as:

$$\sum_{\boldsymbol{j} \in \boldsymbol{J}} q_j w_{jk2} \leq Q_{k2}, \quad \forall k_2 \in K_2 \tag{4}$$

(4) Constraints of Delivery Time: Ensure that the total transit time for primary transport vehicles from distribution centers through transfer hubs to customers' locations falls within customer-specified time windows and can be expressed as:

$$h_j^1 \leq t_{ij}^1 \leq h_j^2, \forall i \in I, \forall j \in J \tag{5}$$

Ensure that the time from secondary carrier departure at transfer hub i to customer point j, plus the time for primary carrier arrival at transfer hub i, meets the time window requirement at customer point j and can be expressed as:

$$h_j^1 - t_{ij}^1 + t_{ij}^2 \leq h_j^2, \forall i \in I, \forall j \in J \tag{6}$$

(5) Constraints of Vehicle Usage: Ensure each Level 1 vehicle serves, at most, one transfer hub and prevent frequent reallocation of vehicles among multiple transfer hubs. This can be expressed as:

$$\sum_{i \in l} Z_{ikl} \leq l, \forall k_l \in K_l \tag{7}$$

Ensure that each secondary transport vehicle serves, at most, one set of customer points (served by the same transfer hub), thus facilitating route planning and scheduling for transport vehicles:

$$\sum_{j \in J} w_{jk2} \leq 1, \forall k_2 \in K_2 \tag{8}$$

3 Design of the Algorithm

3.1 Initialization of Algorithm Parameters

The performance of ant colony algorithms is highly sensitive to parameter settings. A well-balanced combination of parameters can effectively harmonise the algorithm's global search capability with its convergence speed, thereby preventing it from becoming trapped in local optima. Given that this study examines a two-tier logistics network model, where primary and secondary routes differ in node scale, distribution characteristics, and constraints, it is necessary to configure algorithm parameters specifically for each tier. Drawing upon recommended values from classical literature in the field and incorporating multiple preliminary experiments conducted with the case studies in this paper, the final initialisation parameters for the algorithm are presented in Table 3.

Table 3. Algorithm initialization data

Parameter	Level 1 Path	Level 2 Path	Explanation of Meaning
Number of ants m	20–50	10–30	Control parallel search scale
Pheromone factor a	1.5	1.0	Pheromone concentration weight
Heuristic factor β	2.0	2.5	Distance/time window influence weight
Volatility coefficient ρ	0.7	0.8	Pheromone decay rate
Maximum Iteration $T_{\max}$	150	200	Algorithm termination condition

3.2 Path Optimization Processing

The probability that an ant departs from the distribution center and selects transfer station i is:

$$p_i^{\text{first}} = \frac{\tau_{0i}^{\alpha} \cdot (1/d_{oi})^{\beta} \cdot \left(Q1/\sum q_j^{(i)}\right)^{\gamma}}{\sum_{j\in \text{ Unselected Transfer Station}} \tau_{oj}^{\alpha} \cdot (1/d_{oj})^{\beta} \cdot \left(Q1/\sum q_j^{(j)}\right)^{\gamma}} \tag{9}$$

New load utilization factor $\left(Q1/\sum qj^{(i)}\right)$ encourages selecting transfer stations with fuller loads. Each Level 1 truck has a total load capacity of $\leq Q1$. The total demand for assigned transfer stations is recorded via a contraindication table; paths exceeding the capacity are discarded. Level 1 transport time $t_{oi} = d_{0i}/v_1$ requires reserving at least 30 minutes buffer time for Level 2 transport.

The probability that an ant departs from transfer station i and selects customer j:

$$p_i^{\text{second}} = \frac{\tau_{ij}^{\alpha} \cdot (1/d_{ij})^{\beta} \cdot \delta\left(e_j \leq t_{0j} + t_{ij} \leq l_j\right)}{\sum_{k\in\, UnattendedCustomers} \tau_{ik}^{\alpha} \cdot (1/d_{ik})^{\beta} \cdot \delta\left(e_k \leq t_{0i} + t_{ik} \leq l_k\right)} \tag{10}$$

Indicator function δ enables this route only when the customer's time window is satisfied. For each secondary truck with the total load $\leq Q_2$, if $t_{0i} + t_{ij} < e_j$, allow waiting up to e_j (incurring additional waiting costs); if $> l_j$, directly reject the route.

A global update occurs after all ants complete one iteration cycle,

$$\tau_{ij}^{\text{new}} = (1-\rho) \times \tau_{ij}^{old} + \sum_{k=1}^{m} \frac{Q}{C_k} \times \delta \quad (\text{Ants}k \cdot \text{traverse path} \cdot ij) \tag{11}$$

where, C_K is the total cost of ant k (fixed cost of relay stations + two-tier transport cost + carbon emission cost). The lower the cost, the greater the pheromone deposition. Pheromones τ_{0i} on the primary path and τ_{ij} on the secondary path update independently, coupled through the outcomes of relay station location.

3.3 Algorithm Steps

Ant colony optimization (ACO) achieves solution space optimization in path planning by simulating the pheromone interaction mechanism of ant colonies. Its core framework comprises three components: Initializing pheromones, constructing the solution space, and updating pheromones. For optimizing the 2E-LRP in food supply chains, the algorithm design in this paper integrated problem-specific constraints with multi-objective optimization goals. Through symbolic modeling and targeted enhancements, it improved computational efficiency.

The initialization phase involves structured assignment of the pheromone matrix τ_{0i} (primary route: distribution center to transfer station i) and (secondary route τ_{ij}: transfer station i to customer point j).

In Level-1 Path Optimization, for load balancing requirements in transit station site selection, the initial pheromone value is positively correlated with the square root of the total customer demand covered, that is:

$$\tau_{0i}^{(0)} = \tau_0 \cdot \sqrt{\sum_{J\in C_i} q_j} \tag{12}$$

C_i represents the candidate customer set for transfer stations, while q_i denotes customer demand. This assignment strategy guides Ant to prioritize exploring high-demand hubs, thereby enhancing load utilization in primary transportation.

In secondary path optimization, considering the time-sensitive nature of food delivery, the initial pheromone value is positively correlated with the customer time window tightness $1/\left(l_j - e_j + 1\right)$, that is:

$$\tau_{ij}^{(0)} = \tau_0 \cdot \frac{1}{l_j - e_j + 1} \tag{13}$$

This optimization amplifies the exploration priority of tightly constrained customers by compressing the reciprocity of the time window span, thereby reducing the risks of food loss.

In the pheromone update component, the update process dynamically adjusts pheromone distribution through a dual "volatility-enhancement" operation, in order to strengthen the attractiveness of efficient and low-carbon pathways. Under the global volatility rule, pheromones decay exponentially to prevent premature convergence, namely:

$$\tau_{0i}^{t+1} = (1-\rho)\cdot\tau_{0i}^{t} \tag{14}$$

$$\tau_{ij}^{t+1} = (1-\rho)\cdot\tau_{ij}^{t} \tag{15}$$

where, ρ represents the volatility coefficient, dynamic adjustment enables the balancing of global exploration and local exploitation capabilities. For the global optimal solution, the pheromone increment is linked to the comprehensive cost index, namely:

$$\mathrm{D}\tau_{oi} = \frac{Q}{Z^{k^*}\cdot\left(1+\delta\cdot CO_2^{k^*}\right)} \tag{16}$$

$$\mathrm{D}\tau_{ij} = \frac{Q}{Z^{k^*}\cdot\left(1+\delta\cdot CO_2^{k^*}\right)} \tag{17}$$

where, Z^{k^*} represents the total cost, $CO_2^{k^*}$ denotes carbon emissions, and δ signifies the carbon emission weighting factor. This mechanism penalizes high-cost and high-emission pathways, guiding the algorithm toward convergence on the cost-carbon emission Pareto frontier. For hubs not activated, an additional fixed cost decay term $\tau_{0i}^{t+1}\cdot(F_i/\max F_i)$ is applied to suppress the retention of pheromones indicating redundant facility locations.

The overall steps of the algorithm are as follows:

(1) Define Problem Parameters: Determine customer point set C, demand q_j, time window $[e_j, l_j]$, candidate transfer station set T, fixed cost F_i, capacity cap_i, vehicle load capacity Q, transportation cost c, carbon emission coefficient C_{co2}.

(2) Initialize Algorithm Parameters: Ant population size m, maximum iteration count $T_{\max}$, pheromone parameters, carbon emission weighting, etc.

(3) Initialize Information Matrix:

$$\tau_{0i}^{(0)} = \tau_0\cdot\sqrt{\sum_{J_\in C_i} q_j},\quad \tau_{ij}^{(0)} = \tau_0\cdot\frac{1}{l_j - \boldsymbol{e}_j + 1} \tag{18}$$

(4) Primary Path Generation (Distribution Center → Transfer Station): For each ant, initialize the set of available transfer stations $N_0^k = T$ and the payload $\mathrm{Load}_1^k = 0$. Iteratively, select transfer stations:

$$p_{0i}^{k} = \frac{(\tau_{0i})^{\alpha}\cdot(1/d_{0i})^{\beta}\cdot\mu_i^{\gamma}}{\sum_{l\in N_0^k}(\tau_{0l})^{\alpha}(1/d_{0l})^{\beta}\cdot\mu_l^{\gamma}} \tag{19}$$

Among them, $\mu_i = \sum_{j\in c_i} q_j/Q_1$ is selected, then Load_1^k is updated. If overloaded, i is discarded.

(5) Secondary Path Generation (Hub → Customer Point): For each hub, initialize the available customer set $N_i^k = C_i$, payload $\mathrm{Load}_2^k = 0$, and time $t^k = 0$. Iteratively, select customer points:

$$p_{ij}^{k} = \frac{(\tau_{ij})^{\alpha}\cdot(1/d_{ij})^{\beta}}{\sum_{l\in N_i^k}(\tau_{il})^{\alpha}(1/d_{il})^{\beta}} \tag{20}$$

If $q_j \le Q_2 - \mathrm{Load}_2^k$ is satisfied and $\mathrm{t}^k + d_{ij}/v_2 \le l_j$, otherwise $p_{ij}^k = 0$, update the load and time. If the constraints are not satisfied, reset the vehicle.

(6) Objective Function Calculation:

$$Z^k = \sum_{i\in S^k} F_i + \sum_{i\in S^k} d_{0i}\cdot c_1 + \sum_{i\in S^k}\sum_{j\in C_i^k} d_{ij}\cdot c_2 + \delta\cdot c_{\mathrm{co2}}\cdot\left(\sum_{i\in S^k} d_{0i} + \sum_{i\in S^k}\sum_{j\in C_i^k} d_{ij}\right) \tag{21}$$

(7) Pheromone Updates: Volatility Phase $\tau_{0i}^{t+1} = (1-\rho)\cdot\tau_{0i}^{t}, \tau_{ij}^{t+1} = (1-\rho)\cdot\tau_{ij}^{t}$; Enhancement Phase $D\tau_{oi} = \frac{Q}{Z^{k^*}\cdot\left(1+\delta\cdot CO_2^{k^*}\right)}$, $\tau_{0i}^{t+1} = \tau_{0i}^{t+1}$; $(F_i/\max F_i)$ Decay (Transit Station not Enabled).

(8) Termination Condition Check: If the maximum iteration count is reached, output the global optimal solution; otherwise, return to step 2 to continue iteration.

4 Analysis of Site Selection Algorithm Improvement

4.1 Results of Traditional Site Selection Algorithms

By applying the K-means clustering algorithm to the data in Table 4, an initial number of clusters $K = 4$ was selected, with four random initial cluster centers chosen. The clustering results are shown in Figure 2. The first cluster includes 03, 05, 07, 09, 11, 14, 17, 20, 23, 26, 29, 32, and 35, with cluster center (52, 53). The second cluster includes 01, 06, 08, 12, 15, 18, 21, 24, 27, 30, 33, and 36, with cluster center (102, 80). The third cluster includes 02, 04, 10, 13, 16, 19, 22, 25, 28, 31, 34, 37, and 40, with a cluster center at (148, 32). The fourth cluster includes 38, 19, 41, 42, 43, 44, 45, 46, 47, 48, 49, and 50, with a cluster center at (28, 122).

Table 4. Coordinate data graph

Node	X	Y	Demand (kg)	Node	X	Y	Demand (kg)	Node	X	Y	Demand (kg)
1	115	75	37	18	105	88	46	35	50	30	45
2	145	25	58	19	140	45	41	36	98	83	50
3	62	48	44	20	65	35	39	37	142	50	44
4	130	35	32	21	118	82	38	38	25	130	45
5	35	60	52	22	165	38	52	39	40	115	52
6	90	85	51	23	55	58	41	40	135	48	34
7	40	38	33	24	95	65	49	41	18	125	35
8	108	90	40	25	125	20	39	42	35	140	40
9	58	55	47	26	38	62	55	43	10	100	48
10	130	35	47	27	102	95	30	44	22	110	32
11	70	65	36	28	158	10	48	45	50	135	55
12	120	60	53	29	67	42	32	46	28	128	44
13	155	15	55	30	88	78	54	47	32	105	37
14	45	40	50	31	138	30	50	48	15	118	41
15	85	70	35	32	42	50	48	49	45	108	50
16	170	28	36	33	112	68	43	50	20	138	39
17	30	70	42	34	168	40	33				

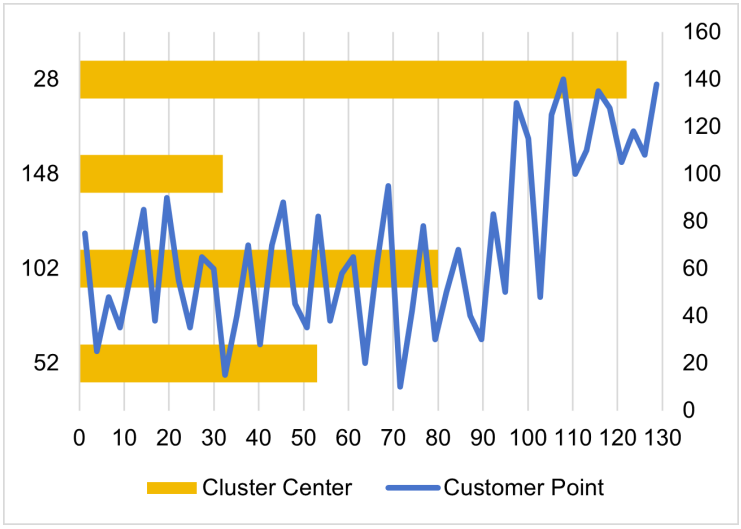

Figure 2. Traditional K-means clustering customer points

The traditional K-means algorithm randomly selects four initial cluster centers, often favoring customer classification based on spatial proximity, which can easily generate anomalous customer points. On the one hand, the random selection of initial cluster centers renders the clustering results sensitive to the initial state. In this experiment, customers who should belong to Cluster 1 were misclassified into Cluster 2. On the other hand, the traditional algorithm does not consider capacity constraints. In the 2E-LRP problem, the total customer demand must not exceed the capacity of the transfer station. However, the traditional algorithm fails to incorporate this factor during clustering, thus causing the total demand of certain clusters to exceed the capacity of the station, resulting in overload anomalies. For example, the total demand of Cluster 3 exceeds the limit, hence complicating route planning and resource allocation while impacting the efficiency of overall logistics distribution. In practical scenarios, to

satisfy the capacity constraint by limiting the total cluster demand to 400 kg, Cluster 5 must be split with its center relocated to (165, 38), to meet the load capacity requirement.

4.2 Improved Site Selection Algorithm Results

This design employed an improved K-means clustering method. First, conduct an inertia analysis: Calculate the inertia values for $K = 2$ to $K = 6$ revealed that the inertia decline rate dropped from 18% to 7% at $K = 4$, thus preliminarily determining $K = 4$. Capacity validation followed: The initial Cluster 3 demanded 450 kg > 400 kg, necessitating forced splitting and ultimately yielding $K = 5$ (with the addition of transfer station C18). K-means++ initialization prioritized the farthest points as initial centers (C01, C05, C08, C10 and C18). The iterative process converged after 2 iterations, with all clusters' demand ≤ 400 kg.

The improved clustering results are shown in Figure 3. The five new cluster centers were (50, 50), (100, 85), (140, 35), (20, 120), and (169, 29). The improved algorithm centers were closer to the theoretical geometric mean. In addition, the pre-splitting of the algorithm enabled the centers of Clusters 3 and 5 to be more reasonable while satisfying the load capacity constraints. By applying the capacity constraint, the improved algorithm reassigned customers C35 to C40 from the original Cluster 3 to Cluster 5. This reduced the demand of Cluster 3 from 540 kg to 260 kg and set the demand of Cluster 5 at 280 kg, in order to satisfy both constraints. This data explicitly demonstrated the advantages of the improved algorithm in selecting the location of a cluster center, particularly its ability to handle capacity constraints, thus resulting in a more reliable layout of the transfer station.

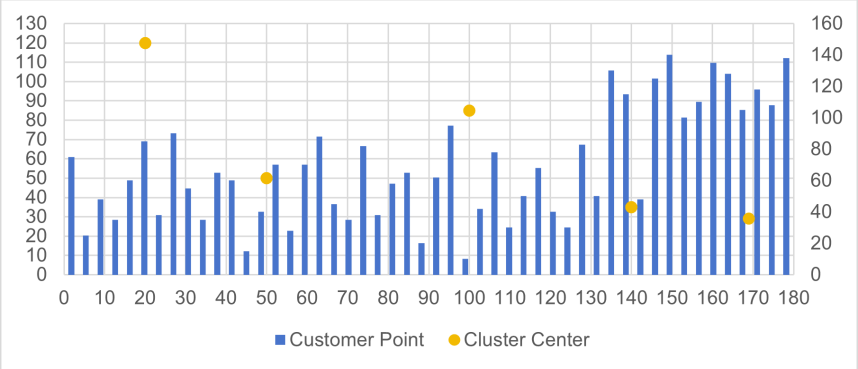

Figure 3. Graph of improved K-means clustering customer classification

4.3 Comparison Analysis before and after Improvement

The following analysis compared three internal metrics of the improved K-means clustering algorithm with those of the traditional K-means algorithm across different-sized datasets, to demonstrate the effectiveness of the improved approach. The three metrics are as follows:

(1) Compactness: Measure the average distance from each sample point within a cluster to its cluster center. The formula is:

$$\text{Compactness} = \sum_{i=1}^{K} \sum_{x \in C_i} \|x - \mu_i\| \tag{22}$$

(2) Separation: Measure the degree of separation between clusters, represented here by the average Euclidean distance between clusters. The formula of the calculation is:

$$\text{Segmentation Degree} = \frac{1}{K(K-1)} \sum_{i=1}^{K} \sum_{j=i+1}^{K} \|u_i - u_j\| \tag{23}$$

(3) Sum of Squared Errors (SSE): The sum of the squared distances between each sample point within a cluster and its cluster center, to emphasize the influence of outliers:

$$SSE = \sum_{i=1}^{k} \sum_{x \in C_i} \|x - \mu_i\|^2 \tag{24}$$

To validate the algorithm's performance, the computational results for the aforementioned metrics were calculated. A comparison of the experimental results is presented in Table 5.

Table 5. Comparison of the experimental results on the effectiveness of the improved K-means clustering algorithm

Example of Calculation	Algorithm	Compactness (km)	Segmentation Degree (km)	SSE (km^2)
C1_2_1	Traditional K-means	12.3	78.3	18200.5
	Traditional K-means	9.8*	85.6*	14850.2*
R2_3_2	Traditional K-means	22.7	62.4	27350.8
	Traditional K-means	18.5*	76.2*	22100.3*
M3_4_3	Traditional K-means	19.1	68.7	21500.6
	Traditional K-means	15.7*	74.5*	17900.9*

Note: Data marked with an asterisk (*) indicates a superior value in the comparison.

After comparison, the following conclusions can be drawn. The improved K-means algorithm, through dynamic K-value, capacity constraints, and high-quality initialization, significantly outperformed the traditional algorithm in compactness, separability, and SSE. The compactness of the improved K-means was lower than that of the traditional K-means. This indicated that in most cases, the distribution within clusters after the improved K-means clustering was denser and the distances between samples were shorter, compared to clusters after traditional K-means clustering and higher similarity within clusters. The separability of all test cases exceeded that of traditional K-means, indicating that the distances between cluster centers in the improved K-means clusters are greater, thus achieving better classification performance, i.e., lower similarity between clusters. The sum of squared errors for all cases was smaller than that of the traditional K-means clustering algorithm, indicating that in the improved K-means clustering results, each sample point within a cluster is closer to its cluster center, resulting in higher intra-cluster similarity. Through the measurement of three internal metrics, it was evident that the improved K-means clustering algorithm achieved superior clustering performance. It is particularly well-suited for scenarios in the food supply chain where high precision in the layout of a transfer station is required, hence effectively reducing redundant distances and resource wastage in subsequent route planning.

5 Performance Validation of the Two-Level Path Planning Algorithm

5.1 Sensitivity Analysis

In ACO , the parameter configuration of the pheromone heuristic factor α, the expectation heuristic factor β, and the pheromone evaporation coefficient ρ directly determines the performance of the algorithm. Among these, α represents the guiding weight of pheromone concentration on path selection. The smaller α, the weaker the guiding effect of the pheromone, making the algorithm prone to random search; an excessively large α amplifies positive feedback, causing the algorithm to prematurely converge to local optima. The β parameter reflects the importance of heuristic information (e.g., path distance): A higher β increases the reliance of an algorithm on prior knowledge, thus reducing its random search capability; conversely, an excessively low β may result in inefficiency due to insufficient guidance. The ρ parameter controls the pheromone evaporation rate: An overly high ρ accelerates pheromone decay, thus compromising algorithm stability; conversely, an excessively low ρ slows pheromone accumulation and impacts convergence speed. Optimally configuring these three parameters is crucial for balancing the global exploration and local exploitation capabilities of the algorithm.

This paper used the Chartered Market Technician (CMT) standard test case vrpnc1 as an example and employed an improved ant colony optimization (IACO) for independent solutions. The performance of the solutions under different combinations of parameters was compared. The results are shown in Table 6.

Table 6. The orthogonal experiment with parameters of the improved ant colony algorithm

Case Number	α	β	ρ	Mean	Optimal Solution	Worst-Case Solution	Extreme Difference	S/N
1	1	1	0.5	482.35	470.12	495.68	25.56	31.24
2	1	3	0.5	465.21	452.34	478.97	26.63	34.57
3	1	5	0.5	450.89	438.76	462.15	23.39	37.82
4	2	1	0.7	475.68	463.21	488.54	25.33	32.71
5	2	3	0.7	445.23	432.05	456.89	24.84	38.56
6	2	5	0.7	438.76	425.53	450.12	24.59	39.15
7	3	1	0.9	502.14	489.32	515.67	26.35	30.58
8	3	3	0.9	490.56	478.21	505.34	27.13	31.89
9	3	5	0.9	482.31	469.87	495.68	25.81	32.45

According to the experimental data in Table 6, when $\alpha = 2, \beta = 5$, and $\rho = 0.7$, the S/N ratio reached 39.15 , representing the globally optimal combination of the parameters. This indicates that the algorithm achieves

maximum stability under this configuration, hence effectively balancing pheromone guidance and heuristic search. When α increased to 3 (cases 7 to 9), the average value rose significantly (e.g., an average of 502.14 km in case 7), thus validating that excessively high pheromone weights could lead to premature convergence. When $\beta = 5$ (cases 3 and 6), the optimal solution significantly outperformed lowscenario β (e.g., the optimal solution of case 3 was 438.76 km versus 470.12 km in case 1), demonstrating that strong heuristic information enhances search accuracy. However, this required moderate $\rho(0.7)$ to prevent excessively slow convergence.

In the comparison of performance, the optimal combination of parameters as in case 6 achieved an average distance of 438.76 km, a 12.6% reduction compared to the worst combination as in case 7. While narrowing the range by 21.8%, significant improvements were noted in solution quality and stability through parameter optimization. The S/N ratio positively correlated with solution quality, where higher signal-to-noise ratios corresponded to lower volatility and higher computational precision. Reasonably adjusting the parameters could effectively avoid local optima, thus enhancing the efficiency and stability of the algorithm in solving 2E-LRP problems in food supply chains. This provided a basis for parameter optimization in subsequent large-scale case studies.

5.2 Algorithm Performance Analysis

This section solved CMT case studies with an IACO algorithm to address vehicle routing problems. Each case underwent six experimental runs, with results rounded to two decimal places. The definitions of the symbols are as follows:

Average: The mean of the six solutions obtained by the improved ant colony algorithm for the vehicle path problem;

Optimum: The minimum value among the six solutions obtained using the improved ant colony algorithm for the vehicle path problem;

BKS: The exact solution obtained by an exact algorithm or the optimum solution obtained by an existing international algorithm;

GAP1: (Average - BKS) / BKS × 100%;

GAP2: (Optimum - BKS) / BKS × 100%;

AVG: Average of GAP1 and GAP2.

For the CMT standard test cases (CMT1 to CMT6), the results obtained from the improved ant colony algorithm are presented in Table 7.

Table 7. Table of the experimental results for the effectiveness of the algorithm

Example of Calculation	Mean	Optimum Value	BKS	GAP1 (%)	GAP2 (%)	AVG (%)
CMT1	325.47	318.23	305.50	6.54	4.16	5.35
CMT2	412.36	405.12	388.70	6.08	4.22	5.15
CMT3	589.72	575.34	550.20	7.18	4.57	5.87
CMT4	632.15	620.45	595.00	6.24	4.28	5.26
CMT5	745.89	730.12	700.50	6.48	4.23	5.35
CMT6	812.34	798.56	765.00	6.19	4.39	5.29

According to the experimental data in Table 7, GAP1 averaged 6.45% and GAP2 averaged 4.31%. This indicates that the IACO algorithm achieves favorable results when solving vehicle routing problems for small-scale and medium-scale test cases. For large-scale test cases, although the influence of local optima under multiple constraints might cause the gap to exceed 8% when compared to the known optimal solution, the algorithm demonstrated a certain degree of stability. Although the GAP was slightly higher in complex cases like CMT3, the overall stability surpassed that of traditional algorithms.

5.3 Validity Analysis

To validate the effectiveness of the improved ant colony algorithm strategy designed in this paper, a comparative analysis was conducted between the improved algorithm and the traditional ant colony algorithm. Ten experiments were performed via six CMT test cases for both algorithms, and the results were then analyzed. The relevant symbols are defined as follows:

MIN1: The minimum value obtained from the ten solutions generated by the traditional ant colony algorithm for the vehicle routing problem.

MIN2: The minimum value obtained from the ten solutions generated by the improved ant colony algorithm for the vehicle routing problem.

AVG1: The average value of the solutions obtained from the ten solutions generated by the traditional ant colony algorithm for the vehicle routing problem.

AVG2: The average value of the solutions obtained by the improved ant colony algorithm for the vehicle routing problem over ten runs.

GAP1: (MIN2 - MIN1) / MIN1 × 100%;

GAP2: (AVG2 - AVG1) / AVG1 × 100%.

Analysis of the experimental data in Table 8 revealed that the improved algorithm achieved a lower MIN2 value than MIN1 across all six test cases, with an average GAP1 of -5.91%. This indicates that dynamic clustering initialization and capacity constraint preprocessing effectively mitigate the impact of local optima. AVG2 decreased by an average of 5.51% compared to AVG1, thus exhibiting lower variability. This reflects that the improved algorithm pheromone update strategy, combining carbon emission and load constraints, converges more efficiently toward high-quality solution spaces. Experimental results demonstrated that the improved ant colony algorithm significantly outperformed the traditional ant colony algorithm in both optimal and average solutions, hence validating the effectiveness of dynamic cluster initialization, capacity constraint verification, and adaptive pheromone update strategies. This enhanced approach exhibits particularly pronounced advantages in complex constraint scenarios (e.g., CMT3 and CMT6), to provide a more efficient solution tool for optimizing green food supply chain networks.

Table 8. The experimental results for the effectiveness of algorithm strategies

Example of Calculation	MIN1	MIN2	AVG1	AVG2	GAP1	GAP2
CMT1	340.50	315.20	355.80	330.10	-7.43	-7.22
CMT2	428.30	402.70	445.60	420.30	-6.07	-5.68
CMT3	595.00	560.80	618.50	585.20	-5.75	-5.39
CMT4	652.40	615.50	675.20	640.30	-5.66	-5.17
CMT5	768.00	725.30	792.30	750.80	-5.56	-5.24
CMT6	835.00	790.60	860.50	815.20	-5.32	-5.26

5.4 Algorithm Comparison Analysis

To validate the performance of the improved ant colony algorithm presented in this paper, ten experiments were conducted using genetic algorithms (GA) and simulated annealing algorithms (SA) across six CMT case studies. The experimental results were then compared and analyzed against those obtained from the improved ant colony algorithm. The relevant symbols are defined as follows:

GA: Average solution obtained by the genetic algorithm after ten iterations for the vehicle routing problem.

SA: Average solution obtained by the simulated annealing algorithm after ten iterations for the vehicle routing problem.

IACO: Average solution obtained by the IACO algorithm after ten iterations for the vehicle routing problem.

GAP1: (IACO-GA) / GA × 100%;

GAP2: (IACO-SA) / SA × 100%;

AVG: Average of all GAP values across all test cases.

The final results are presented in Table 9.

Table 9. Comparison between the improved ACO algorithm and other algorithms

Example of Calculation	GA	SA	IACO	GAP1	GAP2
CMT1	345.21	338.76	318.23	-7.81	-6.06
CMT2	435.67	425.12	405.12	-6.92	-4.70
CMT3	620.45	605.32	575.34	-7.27	-4.95
CMT4	665.12	650.45	620.45	-6.72	-4.61
CMT5	780.56	765.34	730.12	-6.46	-4.60
CMT6	850.12	835.21	790.60	-6.99	-5.34
AVG	–	–	–	-6.91	-4.97

Experimental data demonstrated that across all test cases, the average solutions generated by the improved ACO (IACO) outperformed those from the genetic algorithm (GA) and simulated annealing (SA), thus validating the effectiveness of the proposed improvement strategy. GAP1 achieved an average optimization of 6.91%, indicating the superiority of IACO over GA in solution quality. GAP2 achieved an average optimization of 4.97%, showing consistent improvement of IACO over SA. GA tends to get stuck in local optima under complex constraints, possibly due to difficulties in directly expressing path constraints through its encoding scheme. While the random search of SA can escape local optima, its convergence speed is relatively slow. In contrast, IACO achieves higher efficiency through pheromone guidance. When solving the vehicle routing problem with capacity constraints, the improved

ACO algorithm demonstrates superior overall performance compared to GA and SA. It is especially appropriate for multi-objective constraint scenarios in optimizing food supply chain network from a green perspective.

6 Conclusions

Driven by both the "Dual-Carbon" goals and the global restructuring of supply chains, the logistics industry is accelerating its transition towards greener and smarter operations. The food supply chain, characterized by high carbon emissions, stringent time constraints, and significant wastage, has emerged as a critical focal point for low-carbon transformation. The traditional single-optimization model prioritizing efficiency alone is no longer sufficient to meet sustainable development requirements. Against this backdrop, this paper addressed the core challenges of hub location selection and route planning in food supply chains. It proposed the 2E-LRP collaborative optimization model, which integrates enhanced K-means clustering with adaptive ACO. The efficacy of the algorithm was validated through multiple experimental sets. The research findings, managerial implications, limitations of the study, and future directions are summarized as follows.

6.1 Key Research Findings

Multi-objective collaborative model construction: The developed 2E-LRP model overcomes the limitations of traditional single-cost optimization approaches. It integrates transfer station construction costs, two-tier transport costs, carbon emission costs, and food perishability costs into a unified objective function. Simultaneously, it incorporates key constraints such as transfer station capacity, vehicle load capacity, and customer time windows. This achieves a balance between the economic and environmental benefits of the food supply chain logistics network, in order to provide a quantitative analytical framework for optimizing green food supply chain networks.

Innovation in coupled algorithm framework: The K-means algorithm is enhanced through "dynamic moment of inertia analysis + capacity presplitting verification" so as to resolve issues of sensitive traditional clustering initialization and imbalance of hub load. This improves the precision and equilibrium of distribution node layout. At the route planning level, an enhanced ant colony algorithm incorporates heuristic information on load utilization rates and time window tightness, alongside an optimized pheromone update mechanism. Compared to traditional ant colony, genetic, and simulated annealing algorithms, this approach demonstrates significant advantages in solution quality and stability, hence effectively balancing transport timeliness, cost, and carbon reduction objectives.

6.2 Implications to the Management

Operational Level: Food logistics enterprises may adopt the "inertia moment-based clustering + capacity verification" logic for the selection of hub sites. This approach optimizes node layout by integrating regional customer demand and time-sensitivity requirements, thereby reducing redundant mileage on trunk routes. Concurrently, applying dual-dimensional "load-time window" dispatch rules to last-mile delivery enhances vehicle utilization while preserving the quality of fresh produce as well as minimizing cold chain disruption losses and carbon emissions.

Government Policy Level: Authorities may leverage the model's carbon reduction quantification logic to formulate differentiated green logistics subsidy policies, to offer special incentives to enterprises adopting coordinated "trunk-end" delivery systems that meet the targets of carbon reduction. Utilizing the end-to-end low-carbon framework of the model, regional top-level planning for green food logistics networks can be developed. This helps identify critical carbon reduction nodes to advance the implementation of "Dual-Carbon" goals in the food distribution sector.

Industry Collaboration Level: Organizations of the logistics industry may establish regional public trans-shipment hub sharing platforms based on the collaborative optimization logic of the model. This would integrate the capacity of trunk transport and last-mile delivery resources across the sector, in order to dismantle inter-enterprise resource barriers. Through centralized scheduling to leverage economies of scale, it would drive the transition of the food supply chain from isolated low-carbon points to encompassing green collaborative operations.

6.3 Research Boundaries

This study operated within the defined application boundaries, with its conclusions subject to the following prerequisite assumptions and scenario settings:

Static scenario assumption: The research assumes fixed locations for the distribution centers, transfer stations, and customer points, with vehicle speeds unaffected by traffic congestion, weather, or other external disruptions. It disregards dynamic demand fluctuations and real-time traffic conditions, resulting in deviations from actual logistics scenarios.

Single-demand constraint: The model optimizes solely for the customer requests for "pure delivery", excluding practical scenarios like "pick-up and delivery integration" or "temporary demand insertion". This limits adaptability to complex delivery needs such as on-demand logistics.

Carbon footprint scope limitation: Emission calculations cover only warehousing and transportation phases, excluding food processing, packaging, and waste disposal across the full lifecycle. This prevents a comprehensive assessment of the potential of overall carbon reduction in the supply chain.

Applicable scale of algorithm: The improved algorithm demonstrates stable performance in small-to-medium scale scenarios. However, when applied to ultra-large-scale customer point networks, the balance between the efficiency of algorithm iteration and solution accuracy requires further validation.

6.4 Future Research Directions

Real-time optimization in dynamic scenarios: Integrate Internet of Things (IoT) and BeiDou positioning technologies to incorporate real-time traffic data and dynamic customer demand. Develop a dynamic 2E-LRP model embedded with reinforcement learning algorithms, to enhance adaptive capabilities for real-time adjustments to the layouts of hubs and delivery routes.

Expansion to multi-demand scenarios: Incorporate practical delivery requirements, such as "pick-up/delivery integration" and "temporary demand insertion" into the model to construct an optimization framework for food supply chain logistics handling multiple types of demand, in order to enhance the adaptability of the model in practice.

Development of a full life-cycle carbon reduction model: Expand the scope of carbon footprint measurement by integrating carbon emission data across all stages, i.e., food processing, packaging, warehousing, transportation, and disposal to construct an optimization model for the full life-cycle green food supply chain. This will drive the transition of the supply chain from localized low-carbon practices to systemic low-carbon transformation.

Algorithm optimization for large-scale networks: Address scenarios with an extremely large number of customer points. Introduce distributed computing and parallel algorithms to streamline existing algorithms. This enhances the efficiency of algorithm iteration while maintaining solution quality, thus meeting the optimization demands of large-scale logistics networks at the enterprise level.

Author Contributions

Conceptualization, Y.Y.Z. and Z.Y.L.; methodology, Z.Y.L. and X.H.Z.; validation, Z.Y.L. and X.H.Z.; formal analysis, Z.Y.L.; investigation, X.H.Z., N.N.Z., X.L.L. and Z.Y.G.; data curation, Z.Y.L., X.H.Z., Y.Y.Z., X.L. and Y.X.X.; writing—original draft preparation, Z.Y.L.; writing—review and editing, Y.Y.Z., N.N.Z. and X.L.L.; visualization, X.H.Z.; supervision, Y.Y.Z.; project administration, Y.Y.Z.; funding acquisition, Y.Y.Z. All authors have read and agreed to the published version of the manuscript.

Data Availability

The data used to support the research findings are available from the corresponding author upon request.

Acknowledgements

The authors would like to express sincere gratitude to practitioners in the food supply chain industry and scholars in the field of operations research. Their expertise provided real-world industry operation data and suggestions about professional algorithm optimization for the research on the two-stage location-routing problem in low-carbon food supply chains. The practical experience and academic insights of these experts have effectively enhanced the rationality of the collaborative optimization model and the reliability of the improved algorithm results in this study, thus laying a solid foundation for the successful completion of the research.

Conflicts of Interest

The authors declare no conflicts of interest.

References

[1] M. Nili, M. S. Jabalameli, A. Jabbarzadeh, and E. Dehghani, "An optimization approach for sustainable and resilient closed-loop floating solar photovoltaic supply chain network design," *Comput. Chem. Eng.*, vol. 193, pp. 108 927–108 927, 2025. https://doi.org/10.1016/J.COMPCHEMENG.2024.108927

[2] A. Saeed, M. Jian, M. Imran, G. Freen, and A. U. R. Majid, "Green-resilient model for smartphone closed-loop supply chain network design: A novel four-valued refined neutrosophic optimization," *Comput. Ind. Eng.*, vol. 190, p. 110087, 2024. https://doi.org/10.1016/J.CIE.2024.110087

[3] H. Mirzaee, H. Samarghandi, and K. Willoughby, "Comparing resilience strategies for a multistage green supply chain to mitigate disruptions: A two-stage stochastic optimization model," *J. Clean. Prod.*, vol. 471, pp. 143 165–143 165, 2024. https://doi.org/10.1016/J.JCLEPRO.2024.143165

[4] R. Solanki, D. Kannan, J. D. Darbari, and P. Jha, "Identification and analysis of drivers for carbon regulatory environmental policies implementation in manufacturing supply chain: A zero carbon perspective," *Clean. Logist. Supply Chain*, vol. 11, p. 100150, 2024. https://doi.org/10.1016/J.CLSCN.2024.100150

[5] V. Dohale, P. Ambilkar, S. K. Mangla, and B. E. Narkhede, "Critical factors to sustaileanant innovations for net-zero achievement in the manufacturing supply chains," *J. Clean. Prod.*, vol. 455, p. 142295, 2024. https://doi.org/10.1016/J.JCLEPRO.2024.142295

[6] Y. Peng, Z. Ren, D. Z. Yu, and Y. Zhang, "Transportation and carbon emissions costs minimization for time-dependent vehicle routing problem with drones," *Comput. Oper. Res.*, vol. 176, p. 106963, 2025. https://doi.org/10.1016/J.COR.2024.106963

[7] X. Zhu, Y. Liang, C. Wu, and Y. Xiao, "Vehicle routing perfection for fresh agricultural products distribution under carbon emission regulation and customer satisfaction," *Processes*, vol. 13, no. 3, p. 605, 2025. https://doi.org/10.3390/pr13030605

[8] P. Lou, Z. Zhou, Y. Zeng, and C. Fan, "Vehicle routing problem with time windows and carbon emissions: A case study in logistics distribution," *Environ. Sci. Pollut. Res. Int.*, vol. 31, no. 29, pp. 41 600–41 620, 2024. https://doi.org/10.1007/S11356-024-31927-9

[9] X. Zeng, J. Li, and K. He, "Innovation and challenges of the global green supply chain in the context of a low-carbon transition," *Chin. Sci. Bull.*, vol. 70, no. 4-5, pp. 549–555, 2025. https://doi.org/10.1360/TB-2024-1259

[10] C. Lu and Z. Fang, "Impact of customer digital technology innovation on supplier carbon emissions: The transmission mechanism of the "dual spillover" of supply chain funds and innovation," *West Forum*, vol. 35, no. 1, pp. 84–96, 2025.

[11] Y. Li and H. Niu, "The supply chain transmission effect of carbon emission trading mechanisms—From the perspective of supplier green innovation," *Account. Res.*, no. 3, pp. 82–94, 2025. https://doi.org/10.3969/j.issn.1003-2886.2025.03.007

[12] B. Hu, Z. Liu, H. Guo, and Y. Zhao, "Carbon emission reduction and pricing optimization under government supervision and carbon trading mechanism," *Front. Sci. Technol. Eng. Manag.*, vol. 41, no. 3, pp. 83–89, 2022.

[13] Z. Wang and Y. Zhang, "Impact of coordinated digital and green transformation on green and low-carbon innovation of export enterprises," *Chin. Popul. Resour. Environ.*, vol. 35, no. 7, pp. 47–56, 2025.

[14] F. Yao, Y. Yan, Y. Li, and J. Sun, "Green design and green marketing decisions of supply chain from the perspective of environmental responsibility," *Manag. Rev.*, vol. 36, no. 6, pp. 255–265, 2024. https://doi.org/10.14120/j.cnki.cn11-5057/f.2024.06.019

[15] T. Xie and X. Gao, "Research on the impact of green mergers and acquisitions on the supply chain resilience of heavily polluting enterprises under the "dual carbon" goal," *J. Ind. Technol. Econ.*, vol. 44, no. 8, pp. 118–127, 2025. https://doi.org/10.3969/j.issn.1004-910X.2025.08.012

[16] J. Kong, M. Xie, and H. Wang, "Integrating autonomous vehicles and drones for last-mile delivery: A routing problem with two types of drones and multiple visits," *Drones*, vol. 9, no. 4, p. 280, 2025. https://doi.org/10.3390/drones9040280

[17] R. Nugraha, A. D. Rendragraha, and S. Y. Shin, "Integrated electric ground vehicle and drone with blockchain-driven approach for routing delivery," *Comput. Oper. Res.*, vol. 180, p. 107057, 2025. https://doi.org/10.1016/j.cor.2025.107057

[18] H. Duan, X. Li, G. Zhang, Y. Feng, and Q. Lu, "Elite-based multi-objective improved iterative local search algorithm for time-dependent vehicle-drone collaborative routing problem with simultaneous pickup and delivery," *Eng. Appl. Artif. Intell.*, vol. 139, p. 109608, 2025. https://doi.org/10.1016/j.engappai.2024.109608

[19] T. Fu, S. Li, and Z. Li, "Research on collaborative delivery path planning for trucks and drones in parcel delivery," *Sensors*, vol. 25, no. 10, p. 3087, 2025. https://doi.org/10.3390/S25103087

[20] J. Zhao, Y. Long, B. Xie, G. Xu, and Y. Liu, "A matheuristic solution for efficient scheduling in dynamic truck–drone collaboration," *Expert Syst. Appl.*, vol. 267, p. 126218, 2025. https://doi.org/10.1016/J.ESWA.2024.126218